



Contents lists available at ScienceDirect



Catalysis Today

journal homepage: www.elsevier.com/locate/cattod

Selective oxidation reactions over tri- and tetradeятate oxovanadium(IV) complexes encapsulated in zeolite-Y

Gavin von Willingh, Hanna S. Abbo, Salam J.J. Titinchi*

Department of Chemistry, University of Western Cape, Private Bag X17, Bellville 7535, Cape Town, South Africa

ARTICLE INFO**Article history:**

Received 12 July 2013

Received in revised form 13 August 2013

Accepted 17 September 2013

Available online xxx

Keywords:

Homogenous catalysis

Heterogeneous catalysis

Zeolite-Y

Tri- and tetradeятate Schiff base complexes

Oxovanadium(IV)

ABSTRACT

The preparation and characterization of VO(IV) complexes of 7-amino-5-aza-4-methyl-hept-3-en-2-one and 4,4'-(ethane-1,2-diyl)dinitrilo)dipentan-2-one inside the super cages of zeolite-Y using the flexible ligand method is described. The structures of these encapsulated complexes were established on the basis of various physico-chemical (XRD, BET and TGA) and spectroscopic studies (UV-Vis, FTIR). The results indicate that zeolite-Y can accommodate these complexes in its super cages without hindering or modifying the framework or structure of the zeolite confirming successful encapsulation of the Schiff-bases throughout the voids of zeolite-Y. These encapsulated complexes were screened as heterogeneous catalysts for various oxidation reactions, viz., phenol, benzene, styrene and cyclohexene using H₂O₂ as oxidant. For comparison, the corresponding neat complexes were screened as potential homogeneous catalysts for these oxidation reactions. The homogeneous complexes were found to be more active than the corresponding encapsulated VO(IV) complexes for these oxidation reactions. The results also proved that the heterogeneous systems described here represent an efficient and friendly environmental for these oxidation reactions, having advantages over homogeneous catalysts. In addition they have high turnover frequency values (TOF) and better selectivity than the corresponding homogeneous catalysts.

© 2013 Elsevier B.V. All rights reserved.

1. Introduction

Transition metal complexes of Schiff base ligands have been employed in homogeneous catalysis for various oxidation reactions due to their high activity, homogeneity, reproducibility, selectivity under mild conditions and thus affirm their investigation in organic synthesis [1]. The problems encountered in homogeneous catalytic systems are the catalyst, reactants and products which are in one phase, making catalyst-product separation, catalyst recovery, recycling and reuse difficult [2]. Formation of oxo-dimers and other polymeric species are always possible in homogeneous catalytic systems leading to irreversible catalyst deactivation [3]. These drawbacks have hampered their use by industry. In order to minimize these drawbacks, heterogenization of homogeneous catalysts was developed to overcome these difficulties and has emerged as a focus of research [4–7]. Encapsulation of these homogeneous catalysts in microporous materials such as zeolites is an attractive technique for heterogenization, since no leaching of metal ions or metal complexes were detected since the complex is trapped in the zeolite pores [8]. In addition, zeolite-encapsulated complexes promise better control of selectivity of the reaction and higher stability as a result of reduced dimerization of complexes in the cavity

[9]. Although polymer and inorganic oxide-anchored complexes have been designed and their catalytic activities are as good as homogeneous catalysts, they suffer from leaching of metal complexes from the solid surface [10]. This disadvantage has restricted their commercial use.

The coordination chemistry of vanadium is of great current interest due to its wide application in medicinal, biological and catalytic systems [11]. Oxovanadium complexes have also attracted considerable attention due to their remarkable catalytic activity and displayed good selectivity for the oxidation of various substrates using H₂O₂ as a green oxidant [12,13]. Encapsulation of oxovanadium(IV) complexes inside the super cages of zeolite-Y and oxovanadium-exchanged zeolite has also been investigated which indicated their potential catalytic activity in oxidation reactions [14–16].

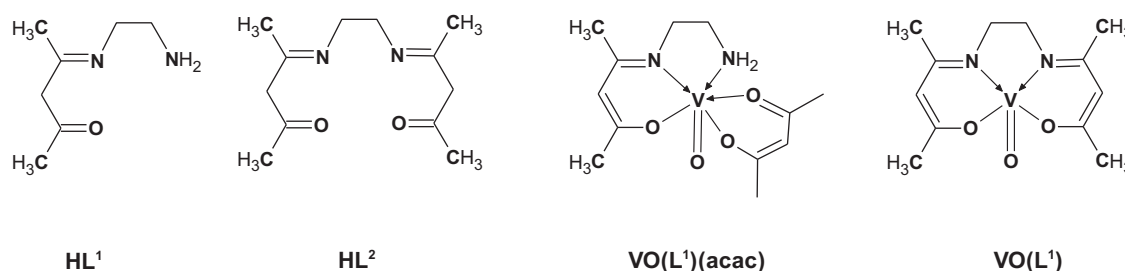
As part of our continuing interest in oxidation reactions by vanadium complexes [15,17,18] and considering the demand of more efficient heterogeneous catalytic systems [19].

We herein report the synthesis and characterization of new heterogeneous oxovanadium catalytic systems, i.e. zeolite-Y encapsulated OV(IV) complexes. These complexes are derived from 7-amino-5-aza-4-methyl-hept-3-en-2-one and 4,4'-(ethane-1,2-diyl)dinitrilo)dipentan-2-one (**Scheme 1**).

Catalytic activities of these complexes have been studied towards the oxidation of phenol, benzene, cyclohexene and styrene. Neat complexes of the above metal ions have also been

* Corresponding author. Tel.: +27 21 959 2217; fax: +27 21 959 3055.

E-mail address: stitinchi@uwc.ac.za (S.J.J. Titinchi).

**Scheme 1.** Structures of the ligands and oxovanadium (IV) complexes.

prepared and their catalytic activities have been compared with the encapsulated ones.

2. Experimental

2.1. Materials

The chemicals were used as received without any further purification. Absolute ethanol (99%) was purchased from Saarchem. Glacial acetic acid and hydrochloric acid (32%) were purchased from Merck. H-Y zeolite was purchased from Zeolyst. Carbon tetrachloride was purchased from Riedel-de Hahn. Dichloromethane (DCM), phenol (99%), hydrogen peroxide (30%), cyclohexene, vanadyl acetylacetone, ethylenediamine, ethyl acetate, acetonitrile, acetylacetone were purchased from Sigma-Aldrich.

2.2. Physical methods and analysis

ATR-IR measurements were carried out on a Perkin-Elmer Spectrum 100 FTIR spectrometer. Electronic spectra were recorded on a GBC UV/VIS 920 UV-Visible spectrophotometer in absolute ethanol or in Nujol (by layering the mull of the sample to the inside of one of the cuvettes while keeping another one layered with Nujol as reference) as well as using diffuse reflectance under ambient conditions. ¹H and ¹³C NMR spectra of ligands were recorded in CDCl₃ solution using a Varian Gemini 2000 spectrometer (¹H at 200 MHz, ¹³C at 50.3 MHz) and chemical shifts are indicated in ppm. Sample signals are relative to the resonance of residual protons on carbons in the solvent. Electrochemical studies were carried out on a BAS 100 B electrochemical analyzer. Three-electrode assembly with Ag/AgCl/KCl (saturated) reference electrode, Pt wire counter electrodes were used. Working electrode consisted of glassy carbon microelectrode (2 mm diameter). All investigations were made of 10⁻² M of sample solutions in dry acetonitrile solution in presence of lithium perchlorate as supporting electrolyte. Each solution was degassed with ultra-pure N₂ gas for 5 min before each measurement was made.

Thermal analysis was measured using Perkin Elmer TGA Q500 Thermobalance. The nitrogen adsorption/desorption and BET surface area was determined at -196 °C using a Tristar 3000 Micromeritics. All samples were degassed prior to the measurement at 120 °C for 12 h. The percentage metal content was determined using ICP-OES Varian 710-ES spectrophotometer. Scanning Electron Micrographs (SEM) of the encapsulated catalysts were recorded on field-emission scanning electron microscopy (Auriga Zeiss SEM) with accelerating voltage: 5 keV. The samples were coated with Au-Pd for 30 s using a Quorum Q150T ES sputter coater to prevent surface changes and to protect the surface material from thermal damage by the electron beam. The powder X-ray diffraction was recorded on a Bruker AXS D8 Advance, High-Resolution diffractometer with Cu K_α Radiation ($\lambda = 1.5406 \text{ \AA}$) fitted with a PSD Vantec gas detector at Ithemba labs, Cape Town, South Africa. All catalysis reaction products were

analyzed using Agilent 7890 gas chromatograph fitted with flame ionization detector and HP-5 phenylmethylsilicon capillary column (30 m × 330 pm × 0.25 μm). The retention time of all the peaks were compared with authentic samples.

2.3. Preparations

2.3.1. 7-Amino-5-aza-4-methyl-hept-3-en-2-one, HL¹

7-Amino-5-aza-4-methyl-hept-3-en-one was synthesized according to a method described by Styring et al. with slight modifications [20]. A cooled solution of ethylenediamine (0.3 g, 0.005 mol) in (25 ml) DCM was added dropwise to a cooled solution of acetylacetone (0.5 g, 0.005 mol) in (25 ml) DCM at 0 °C under stirring conditions at ambient temperature. The solution was stirred for 5 min and refluxed for an additional 5 min at 40 °C. Afterwards, the solvent was removed *in vacuo* to give viscous oil. Yield = 0.97 g (68%).

¹H NMR δ ppm (CDCl₃, 200 MHz): 1.48 (s, 6H, CH₃), 1.56 (s, 2H, NH₂), 2.46 (m, 2H, CH₂), 3.42 (m, 2H, CH₂), 4.58 (s, 1H, =C—H), 10.45 (br, 1H, OH).

2.3.2. 4,4'-(Ethane-1,2-diyl)dinitrilo)dipentan-2-one, HL²

4,4'-(Ethane-1,2-diyl)dinitrilo)dipentan-2-one was synthesized according to literature procedure [21]. A solution of acetylacetone (2 g, 0.02 mol) in 25 ml DCM was added dropwise to a solution of ethylenediamine (0.6 g, 0.01 mol) in 25 ml DCM under stirring conditions. After addition, the pH of the solution was adjusted to 6 with a few drops glacial acetic acid. The yellow solution was refluxed for 3–4 h at 40 °C. Afterwards, the solvent was removed *in vacuo* and gave a yellow solid. The solid product was recrystallized by dissolving it in a 1:1 mixture of ethylacetate and DCM by heating. After recrystallization from the same solvent and twice from CCl₄ the product was filtered and air dried to give straw like crystals. Yield = 2.07 g (55.6%); m.p. = 111–113 °C. ¹H NMR δ ppm (CDCl₃, 200 MHz): 1.88 (s, 6H, CH₃), 1.95 (s, 6H, CH₃), 3.43 (m, 4H, CH₂), 4.97 (s, 2H, =C—H), 10.86 (br, 2H, OH).

2.3.3. Oxovanadium(IV) complexes

A hot solution of VO(acac)₂ (0.265 g, 0.001 mol) in ethanol (10 ml) was added dropwise to ethanolic solution (10 ml) of the appropriate ligand (HL¹ or HL²) (0.001 mol). The reaction mixture was heated and stirred under reflux for 5 h. The complex slowly separated out from filtered, and the solid was washed with hot water followed by ethanol and dried at 100 °C. Recrystallization from MeCN gave analytically pure products.

VO(L¹)(acac): light green solid, yield 0.20 g (65.5%); m.p. > 300 °C and

VO(L²): green powder, yield 0.18 g; (61.7%); m.p. 235–237 °C (Lit. 236 °C [22]).

2.3.4. Oxovanadium(IV) exchanged zeolite, VO-H-Y

To 1.0 g H-Y suspended in 50 ml deionized water was added VO(acac)₂ (0.53 g, 2 mmol). The reaction mixture was stirred at 90 °C

Table 1

FT-IR spectral data of the ligands and VO(IV) complexes.

| Compound | ν (cm ⁻¹) | | | |
|-----------------------------|---------------------------|---------------|------------------|------------|
| | | (C=N) | $\nu(M-O)/(M-N)$ | $\nu(V=O)$ |
| HL ¹ | 1602(s) | – | – | – |
| HL ² | 1599(s) | – | – | – |
| [VO(L ¹)(acac)] | 1570(s) | 386, 408, 485 | 978 | – |
| [VO(L ²)] | 1559(s) | 418, 481 | 970 | – |

for 24 h, filtered, washed with copious amounts of hot deionised water followed by Soxhlet extraction with acetonitrile for 3 h. The resulting precipitate was dried at 150 °C in air for 24 h.

2.3.5. Synthesis of zeolite-Y encapsulated metal complexes

OV-H-Y zeolite (0.3 g) and ligand (0.7 g) were mixed in MeCN (30 ml) and the reaction mixture was refluxed with stirring overnight. The resulting material was collected by filtration and was subsequently Soxhlet extracted in MeCN for 48 h. The solid residue obtained was dried at 120 °C in air for several hours.

2.4. Catalytic activity

2.4.1. Catalytic liquid phase oxidation reaction

Catalytic liquid phase oxidation reactions were carried out in a 50 ml round-bottom flask fitted to a water condenser. In a typical reaction, equimolar amounts of substrate and 30% H₂O₂ were mixed in 3 ml MeCN and the reaction mixture was refluxed and stirred in an oil bath at 70 °C after which the catalyst (0.01 g) to be tested was added and this was assumed to be the starting point of the reaction. Progress of the reaction was monitored as a function of time by withdrawing small aliquots after certain time intervals and analysing them quantitatively by gas chromatograph.

2.4.1.1. Hydroxylation of phenol. Phenol (2.35 g, 0.025 mol), 30% H₂O₂ (2.83 g, 0.025 mol) and catalyst (0.01 g) were mixed in 3 ml of MeCN at 70 °C.

2.4.1.2. Oxidation of benzene. Benzene (1.95 g, 0.025 mol), 30% H₂O₂ (2.83 g, 0.025 mol) and catalyst (0.01 g) were mixed in 3 ml MeCN at 70 °C.

2.4.1.3. Oxidation of cyclohexene. Cyclohexene (2.05 g, 0.025 mol), 30% H₂O₂ (2.83 g, 0.025 mol) and catalyst (0.01 g) were mixed in MeCN (3 ml) at 70 °C.

2.4.1.4. Oxidation of styrene. Styrene (2.60 g, 0.025 mol), 30% H₂O₂ (2.83 g, 0.025 g) and catalyst (0.01 g) were mixed in 3 ml of MeCN at 70 °C.

3. Results and discussion

3.1. Characterization of catalysts

3.1.1. IR spectral studies

The major IR spectral data of the ligands and complexes are presented in **Table 1**. Comparisons of the spectra of these complexes with their respective ligands provide evidence for involvement of the ligand in complex formation. The $\nu(C=N)$ band is shifted to lower wavenumbers indicating the involvement of azomethine nitrogen in coordination to V(IV) metal centre. Disappearance of the weak broad band, $\nu(OH)$, in both neat complexes confirmed participation of the OH group indicating its deprotonation followed by coordination to the metal ion. Bonding of metal ions to the ligands through the nitrogen and oxygen atoms is further supported by the presence of new bands in the 400–600 cm⁻¹ region due to

Table 2

Electronic spectral data of ligands and VO(IV) complexes.

| Ligand/complex | λ_m/nm |
|-----------------------------|--|
| HL ¹ | 202, 302 ^{sh} , 316 |
| HL ² | 202, 303 ^{sh} , 322 |
| VO(L ¹)(acac) | 202, 241 ^{sh} , 308, 347, 773 |
| VO(L ¹)(acac)-Y | 201, 319, 373, 607 |
| VO(L ²) | 202, 266 ^{sh} , 302, 320 ^{sh} , 562, 750 |
| VO(L ²)-Y | 204, 318, 618 |

the $\nu(M-O)$ and $\nu(M-N)$ modes, respectively [23]. Neat complexes exhibit a medium-sharp band around 978–970 cm⁻¹ due to $\nu(V=O)$ stretch [17,18,24]. The FTIR patterns of all guest–host catalysts are very similar and are dominated by the strong bands due to vibrations of the zeolite. These characteristic bands corresponding to the zeolite framework in all samples are found around at 1050, 450, 780 and 394 cm⁻¹.

No shift or broadening in the structure sensitive band at 1050 cm⁻¹ (due to an asymmetric T–O stretch) occurred demonstrating that little change in the zeolite framework upon encapsulation or ion exchange occurred indicating that there is no significant expansion of the zeolite cavity nor dealumination thus proving that the metal complex fits in the cavity of the zeolite and that the zeolite matrix remains unchanged [25–27].

The intensity of IR bands in both zeolite encapsulated complexes is weak in comparison to those of the free metal complexes due to low concentration of the complexes in zeolite cavities.

3.1.2. UV-Vis spectral studies

Table 2 presents the electronic spectral data of ligands, complexes and the corresponding encapsulated complexes. Both ligands exhibit bands at 202, 302 and ~320 nm are assigned to $\Phi \rightarrow \Phi^*$, $\pi \rightarrow \pi^*$ and $n \rightarrow \pi^*$ transitions, respectively. These bands shifted to lower energy on complexation indicating the coordination of the ligands to metal ion [15].

This coordination is further supported by the appearance of a lower intensity band at 347 and 320 nm in VO(L¹)(acac) and VO(L²), respectively, due to ligand to metal charge transfer (LMCT) transition. In addition, both neat complexes display new broad bands in the region 562–773 nm due to the expected d-d transitions (**Fig. 1**).

The spectra of oxovanadium(IV) complexes are characterized by three d-d transitions according to the energy level scheme by Ballhausen and Gray [28].

The encapsulation of the oxovanadium complexes is further supported by the appearance of d-d transitions. Both encapsulated complexes exhibit d-d bands in the visible region at

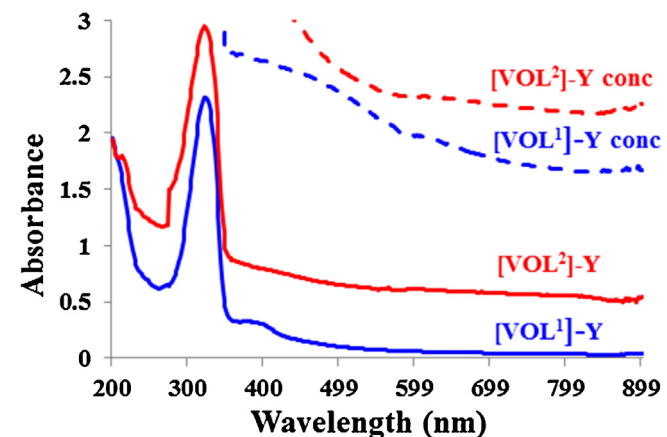


Fig. 1. Electronic spectra of the encapsulated complexes in different concentration.

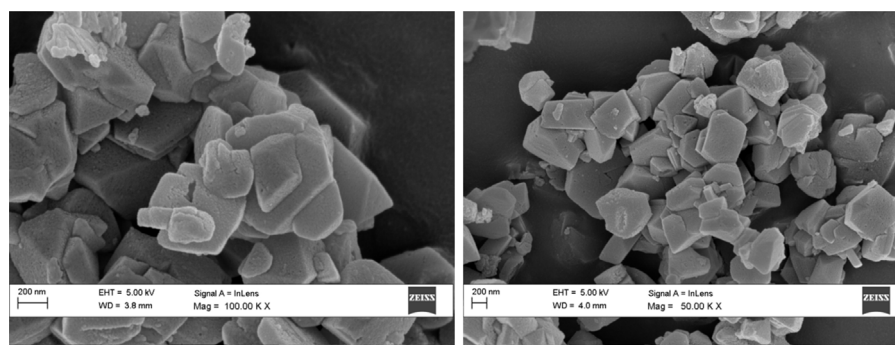


Fig. 2. High resolution scanning electron mircographs of VO-Y (left) and VO(L1)(acac) (right).

607–618 nm which are assigned to band I ($d_{xy} \rightarrow d_{xz}, d_{yz}$) and band II ($d_{xy} \rightarrow d_{x^2-y^2}$).

The third expected transition ($d_{xy} \rightarrow d_z^2$) usually merged with the strong CT band [23,29].

3.1.3. Scanning electron microscopy of OV(VI) encapsulated complexes

The Scanning Electron Micrograph (SEM) of the metal-exchanged zeolite and their respective encapsulated complexes indicate the presence of well-defined zeolite crystals without any shadow of metal ions or complexes present on their external surface (Fig. 2). This confirms that the zeolite preserves its morphology and structure upon encapsulation of complexes. This indicates that Soxhlet extraction is an excellent way for the removal of uncomplexed ligands and complexes from the zeolite surface.

3.1.4. Thermal analysis

Thermogravimetric analyses (TGA) data of the encapsulated complexes along with the percent mass loss at different steps are presented in Fig. 3. $[VOL^1(\text{acac})]-Y$ shows four stage losses. The first step occurs at temperature 150 °C with 2 wt% loss due to the presence of trapped water or physically adsorbed water. The second decomposition step at 150–220 °C refers to the loss of intra-zeolite water molecules (1%), i.e. chemisorbed water in the form of OH groups in zeolite-Y [30].

The third decomposition step (250–330 °C) with 1.5% weight loss is due to the loss of coordinated acetyl acetone molecule. The rest of the organic ligand decomposes in the final step in a wide range (330–650 °C). The thermal decomposition of the encapsulated complex $[VOL^2]-Y$ shows a three-stage loss in the TGA trace. A very small percent weight loss (2%) in the final step which took place over a wide range of temperature is assigned to the loss of the chelating ligand indicating the presence of only small amounts

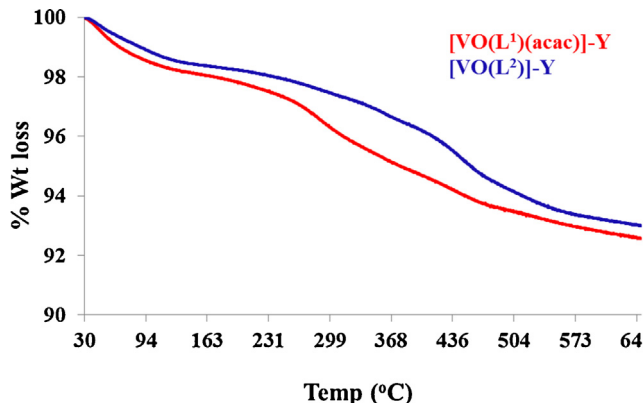


Fig. 3. TGA thermograms for the encapsulated complexes.

of metal complex in the cavity of the zeolite. This is in agreement with the low percent metal content estimated by ICP.

3.1.5. X-ray powder diffraction studies

The X-ray powder diffraction (XRD) patterns of H-Y, OV-Y and their encapsulated complexes in zeolite are presented in Fig. 4. XRD patterns of the zeolitic host before and after complex formation indicates no remarkable differences, although a slight change in intensity of these typical lines in the encapsulated complexes was noticed. This confirms that metal exchange and encapsulation of complexes have little influence on the crystallinity and that the zeolite host can accommodate these complexes. The diffraction pattern for the metal or complexes could not be detected in the encapsulated complexes. This could possibly be due to low loading of metal complexes present in the zeolite.

3.1.6. Surface textural studies

The surface textural properties for the zeolite encapsulated complexes are presented in Table 3. Clearly, inclusion of VO(IV) Schiff base complex in the zeolite cavities considerably reduced the pore volume and the surface area of the zeolite host. This confirms the existence of VO(IV) complexes in the zeolite cavities rather than on the external surface [31]. The decreasing values in the surface area, pore volume and adsorption capacity depends on the amount of incorporated complexes as well as their molecular size and geometrical conformation inside the zeolitic host.

Fig. 5 shows the N_2 adsorption/desorption isotherms and pore size distribution for VO-Y and their respective encapsulated catalysts, which are typical type I according to the IUPAC classification

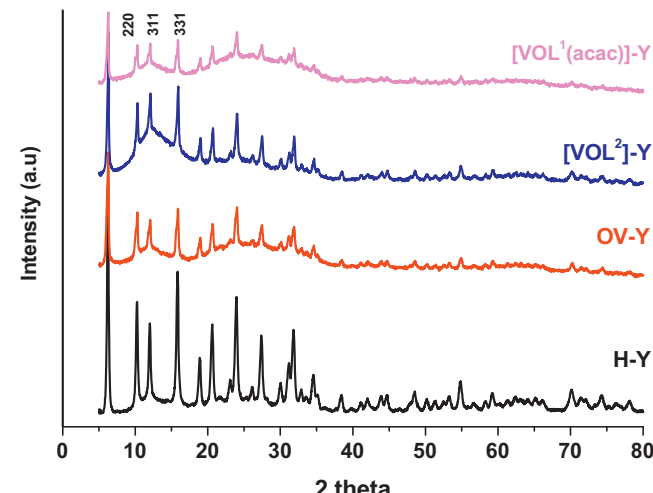


Fig. 4. XRD patterns of H-Y, OV-Y, $[VOL^1(\text{acac})]-Y$ and $[VOL^2]-Y$.

Table 3

Analytical data and surface area and pore volume data for the catalysts and their parents' analogues.

| Catalyst | %V content (% wt) | BET surface area (m^2/g) | Pore volume (ml/g) | Average pore size (Å) |
|-------------------------------|-------------------|--|--------------------|-----------------------|
| H-Y | – | 780 | 0.48 | 42.50 |
| OV-H-Y | 0.28 | 535 | 0.41 | 31.01 |
| [VO(L ¹)(acac)]-Y | 0.11 | 518 | 0.40 | 30.47 |
| [VO(L ²)]-Y | 0.12 | 524 | 0.40 | 30.46 |

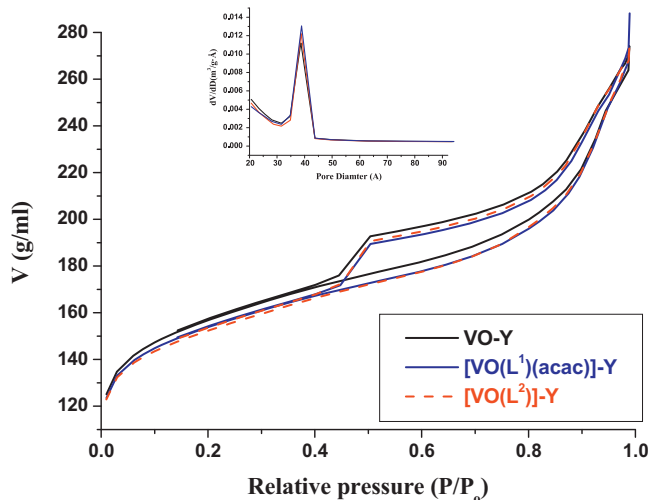


Fig. 5. N_2 adsorption/desorption isotherms VO-Y, $[\text{VO}(\text{L}^1)(\text{acac})]\text{-Y}$ and $[\text{VO}(\text{L}^2)]\text{-Y}$ and pore size distribution pore diameter (inset).

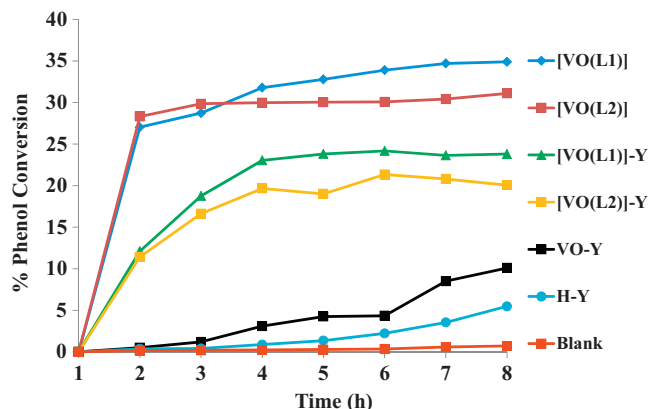


Fig. 6. Kinetic plot for phenol conversion over various catalysts. Reaction conditions: Phenol 2.35 g, H_2O_2 2.83 g, catalyst 10 mg, CH_3CN 3 ml, 70 °C.

and are characteristics of the microporous nature of the materials. This supports the observation that the complexes are present within the zeolite cages and not on the external surface since the zeolite crystallinity was retained.

3.2. Catalytic activity studies

The synthesized catalysts were screened for various oxidation reactions under optimized reaction conditions [19,32].

3.2.1. Oxidation of phenol

The catalytic activities and product selectivity of encapsulated VO(IV) complexes and their neat complexes along with its parent compounds for the oxidation of phenol are represented in Fig. 6 and Table 4. The liquid-phase hydroxylation of phenol using these catalysts and H_2O_2 as an oxidant was studied as a function of time.

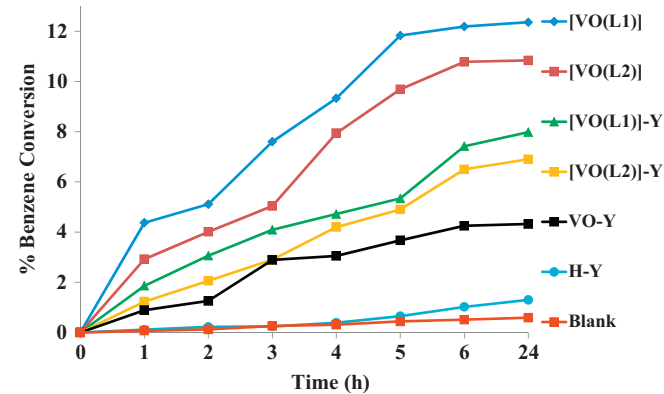


Fig. 7. Kinetic plot for benzene conversion over various catalysts. Reaction conditions: Benzene 1.95 g, H_2O_2 2.83 g, catalyst 0.01 g, CH_3CN 3 ml, 70 °C.

Two products catechol and hydroquinone were observed with a mass balance of >95%.

Blank experiments performed without the catalyst show <1% conversion. The use of H-Y zeolite as catalyst resulted in a 3.5% phenol conversion showing the ineffectiveness of zeolite framework to catalyze the reaction. However, in the case of V-exchanged zeolite the conversion of phenol was higher than the parent H-Y zeolite. Our results in the oxidation of phenol demonstrate the catalytic potential of neat and encapsulated VO(IV) complexes, demonstrating the higher conversion in comparison to VO-Y. This indicates that the presence of the ligand in the complex significantly increase its catalytic activity in comparison to VO-Y. It also indicates that the changes in electronic environment about the central vanadium ions influence the catalytic performance by 10%. This also serves as evidence for the successful complexation of VO(IV) ions with HL¹ or HL² ligands inside the zeolitic host.

Fig. 6 shows that % phenol conversion for the encapsulated catalysts increases considerably within 2 h reaching a steady state after 3 h. The encapsulated catalysts exhibit similar conversion to the neat complexes. However, the TOF values for the heterogeneous catalysts were much higher than the homogenous systems by more than 100-fold.

In terms of selectivity the heterogeneous catalysts were more selective for CAT formation compared to the homogeneous reaction. In both homogeneous and heterogeneous catalysts, the selectivity towards catechol predominated.

3.2.2. Oxidation of benzene

The results of the conversion of benzene over time for various catalysts at 70 °C and in the absence of catalyst are illustrated in Fig. 7. The reaction proceeds selectively for formation of phenol, since no other products were detected. Using $[\text{VO}(\text{L}^1)(\text{acac})]\text{-Y}$ and $[\text{VO}(\text{L}^2)]\text{-Y}$, benzene conversion is 7.4 and 6.5% with TOF value of 1413 and 1138, respectively. On the other hand, compared with the corresponding heterogeneous catalysts, the neat complexes, $[\text{VO}(\text{L}^1)(\text{acac})]$ and $[\text{VO}(\text{L}^2)]$ showed higher conversion of 12.2 and 10.8% with TOF values of 16 and 13, respectively.

Oxidation of benzene catalyzed by VO-Y and H-Y was also attempted to investigate the active site for heterogeneous catalysts

Table 4% Phenol conversion,^a product selectivity and TOF values.

| Catalyst | % Phenol conversion | % Product selectivity | | CAT/HQ | TOF (h ⁻¹) |
|-------------------------------|---------------------|-----------------------|------|--------|------------------------|
| | | CAT | HQ | | |
| [VO(L ¹)(acac)] | 34.7 | 50.7 | 49.3 | 1.0 | 45 |
| [VO(L ²)] | 30.4 | 53.0 | 47.0 | 1.1 | 37 |
| [VO(L ¹)(acac)]-Y | 23.6 | 65.2 | 34.8 | 1.9 | 4554 |
| [VO(L ²)]-Y | 20.8 | 59.6 | 40.4 | 1.5 | 5377 |
| VO-Y | 8.5 | 81.0 | 19.0 | 4.3 | 644 |
| H-Y | 3.5 | 95.8 | 4.2 | 22.8 | — |
| Blank | 0.6 | 94.2 | 5.8 | 16.2 | — |

^a Reaction conditions: phenol 2.35 g, H₂O₂ 2.83 g, catalyst 10 mg, CH₃CN 3 ml, 70 °C, 6 h.

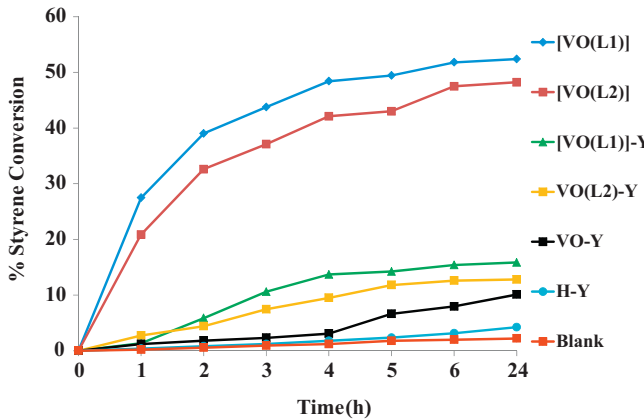


Fig. 8. Kinetic plot for styrene conversion over various catalysts. Reaction conditions: Styrene 2.60 g, H₂O₂ 2.83 g, 0.010 g catalyst, CH₃CN 3 ml, 70 °C.

and gave phenol (1.0–4.3%) that was lower than when encapsulated complexes was utilized. The TOF value for the OV-Y was 323. Less than 1% phenol was detected in the absence of catalyst (blank reaction). This also substantiates the presence of transition metal complexes that are the active site and not the vanadium ions in zeolite.

3.2.3. Oxidation of styrene

The catalytic oxidation of styrene using the neat and the corresponding encapsulated complexes was studied and results are presented in Table 5 and Fig. 8. [VO(L¹)(acac)]-Y and [VO(L²)]-Y catalysts showed 15.4 and 12.6% conversion of styrene after 6 h, respectively. As shown in Table 5, oxidation of styrene was more prominent with neat metal complexes in comparison to encapsulated metal complexes. This could be due to diffusion resistance of styrene molecules through the zeolite windows [33].

Although conversion of styrene using encapsulated catalysts is distinctly low, the selectivity for benzaldehyde is much higher than that of the neat complexes. This may be due to the acidic nature of the zeolite matrix that leads to styrene epoxide ring opening [34]. In general, styrene oxidation gave benzaldehyde as the predominant product which may be due to over oxidation of styrene oxide by nucleophilic attack by H₂O₂ [35] or through direct oxidative cleavage of the styrene side chain double bond by a radical reaction mechanism [36]. Formation of 1-phenylethane-1,2-diol is possibly due to hydrolysis of styrene oxide and to the oxidation of styreneoxide by a nucleophilic attack of hydroperoxy species on styreneoxide, followed by cleavage of the intermediate hydroperoxystyrene. Formation of other products, e.g. phenylacetaldehyde could be through isomerization of styrene oxide and is a much slower process. Other products such as phenylacetaldehyde may form through further oxidation of benzaldehyde or through isomerization of styreneoxide. Therefore, the presence of styrene oxide

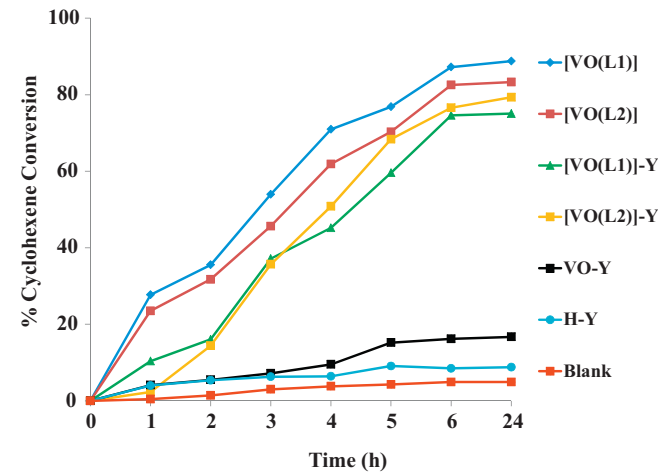


Fig. 9. Kinetic plots for cyclohexene conversion over various catalysts. Reaction conditions: Cyclohexene 2.06 g, H₂O₂ 2.83 g, catalyst 10 mg, CH₃CN 3 ml, 70 °C.

in low yield is more likely. Blank experiment in the absence of catalyst and in the presence of oxidant under the same experimental conditions was negligible for the oxidation of styrene suggesting that the activity of the encapsulated catalysts is mainly due to the presence of the metal complexes in the zeolite cavities.

Significant increases in the performance of these catalysts were observed on increasing the reaction time and level-off after 3 h. Further increase in reaction time slightly enhanced the catalysts' performance.

Although the styrene conversion was higher with the neat complexes, the TOF values for the heterogeneous catalysts were much higher than that of the homogenous analogues.

3.2.4. Oxidation of cyclohexene

Fig. 9 presents the % cyclohexene conversion details as a function of time in the presence of various catalysts as well as in the absence of catalyst. Table 6 summarizes the % conversion of cyclohexene for these catalysts and the selectivities for the various reaction products. As depicted in Fig. 9, both the homogeneous and heterogeneous catalysts were efficient in cyclohexene oxidation providing good yields. Encapsulated catalysts led to high conversions reaching values up to 75–77% whereas, the neat complexes showed a higher conversion rate of cyclohexene into products than of their encapsulated analogues (83–87%).

In terms of selectivity, the % yield for cyclohexene oxide is quite satisfactory (25–39%). It has been reported that H₂O₂ gives much better epoxidation results than *tert*-butyl hydroperoxide (TBHP). With H₂O₂, the oxidation occurs mostly on the double bond giving cyclohexene oxide in good yields, while TBHP promotes the allylic pathway [37]. The formation of the allylic oxidation products 2-cyclohexene-1-one and 2-cyclohexene-1-ol shows the

Table 5Styrene conversion,^a product selectivity and TOF values.

| Catalyst | % Styrene conversion | % Product selectivity | | | | | TOF (h ⁻¹) |
|-------------------------------|----------------------|-----------------------|----------|------|-----------|--------|------------------------|
| | | Bzald | Phacetal | StyO | PhEt diol | Bzacid | |
| [VO(L ¹)(acac)] | 51.8 | 51.7 | 7.2 | 1.5 | 1.0 | 38.6 | 67 |
| [VO(L ²)] | 47.5 | 51.0 | 4.9 | 0.1 | 1.7 | 42.3 | 57 |
| [VO(L ¹)(acac)]-Y | 15.4 | 75.9 | 6.1 | 6.7 | 6.2 | 5.1 | 2972 |
| [VO(L ²)]-Y | 12.6 | 78.3 | 3.6 | 6.2 | 2.3 | 9.6 | 2229 |
| VO-Y | 8.0 | 89.6 | — | 10.4 | — | — | 606 |
| H-Y | 3.2 | 86.8 | 3.1 | 6.9 | 3.2 | — | — |
| Blank | 2.0 | 89.7 | 3.1 | 3.8 | 3.4 | — | — |

^a Reaction conditions: styrene 2.60 g, H₂O₂ 2.83 g, 0.010 g catalyst, CH₃CN 3 ml, 70 °C, 6 h.**Table 6**Cyclohexene conversion,^a product selectivity and TOF values.

| Catalyst | % Cyclohexene conversion | % Product selectivity | | | | TOF (h ⁻¹) | |
|-------------------------------|--------------------------|-----------------------|------|-------|--------|------------------------|--------|
| | | CyOx | CyOl | CyOne | CydiOl | | |
| [VO(L ¹)(acac)] | 87.2 | 28.4 | 46.0 | 21.7 | 2.5 | 1.3 | 112 |
| [VO(L ²)] | 82.6 | 29.0 | 34.6 | 33.4 | 1.3 | 1.8 | 100 |
| [VO(L ¹)(acac)]-Y | 74.6 | 25.4 | 24.8 | 48.3 | 1.7 | 0.2 | 14,465 |
| [VO(L ²)]-Y | 76.6 | 41.2 | 26.2 | 35.6 | — | — | 13,615 |
| VO-Y | 16.0 | 25.4 | 24.8 | 48.3 | 1.7 | 0.2 | 1219 |
| H-Y | 8.5 | 49.9 | 12.9 | 16.5 | 6.1 | 4.7 | — |
| Blank | 4.9 | 53.1 | 28.1 | 12.9 | 2.9 | 3.1 | — |

^a Reaction conditions: cyclohexene 2.06 g, H₂O₂ 2.83 g, catalyst 10 mg, CH₃CN 3 ml, 70 °C.

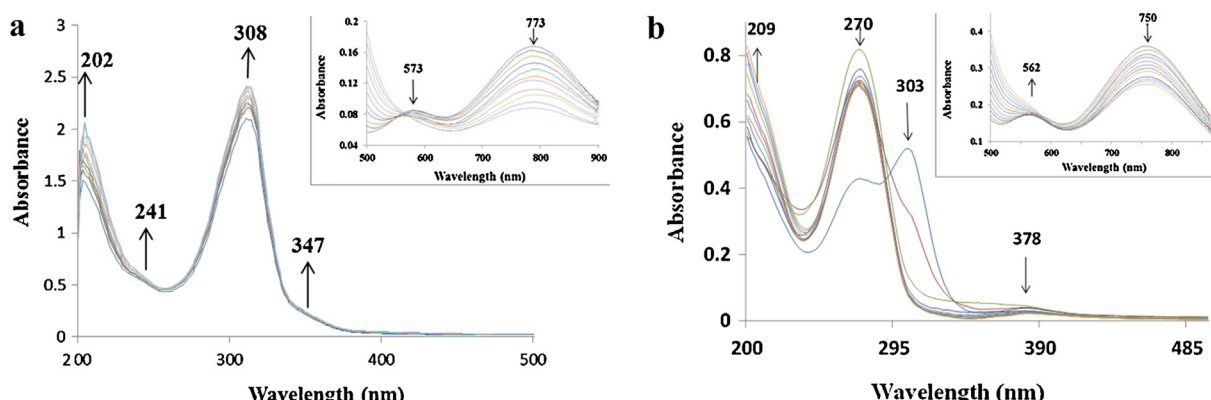
preferential attack of the activated C–H single bond over the C=C double bond. It seems that the diol product resulted from the epoxide ring opening under the aqueous acidic conditions. Furthermore, the cyclohexene conversion was relatively low around 4.9–8.5% in the absence of the catalyst or H-Y. These results have clearly indicated that an enhancement in the conversion percentages in the presence of the neat and the encapsulated catalysts confirm the determining role played by metal complexes encapsulated in the zeolite [38].

3.2.5. Stability and recyclability of the catalyst

The stability and reusability of the encapsulated catalysts were investigated for the oxidation of phenol. The catalyst was recovered by filtration and regenerated by Soxhlet extraction (MeCN), dried at 150 °C for 6 h and reused for two consecutive runs. The recycled catalyst was found to exhibit comparable activity and selectivity with that for the fresh catalysts under the same reaction conditions. The % conversion was lowered by 2–3% but reserved its selectivity. On the other hand, the oxidation did not continue after removal of the catalyst from the reaction mixture, thus confirming the necessity of the catalyst for the reaction to proceed and that no leaching of vanadium species from the catalyst had occurred.

3.3. Possible reaction pathway of catalysts

In order to better understand the reaction pathway and intermediate species formed during oxidation of the substrates, we monitored the progress of the reaction using electronic absorption spectroscopy by treating a methanolic solution of the neat VO(IV) complexes with a methanolic solution of H₂O₂. As shown in Fig. 10a, addition of a methanolic solution of H₂O₂ dropwise to a 10⁻⁴ M methanolic solution of VO(L¹)(acac) resulted in slight increase in the intensities for the bands at 202, 241, and 308 nm, while the intensity of the band at 374 nm remained constant without changing their positions. On the other hand, the dropwise addition of methanolic H₂O₂ to 10⁻³ M methanol solution of VO(L¹)(acac) resulted in spectral changes in the visible region and is depicted in Fig. 10a (inset). The d–d band in VO(L¹)(acac) at 773 and 573 nm were decreased in intensity and the band 573 nm was disappeared with further addition of H₂O₂. These changes are due to the generation of oxoperoxovanadium(V) species [39], where the peroxy complex, thus formed, transfers one of its oxygens to the substrate during oxidation. Disappearance of the d–d band and the appearance of the isosbestic point suggests the transformation of OV(IV) complex into a peroxy species.

**Fig. 10.** UV–Visible spectral studies of (a) VO(L¹)(acac) and (b) VO(L²) after the successive dropwise addition of methanolic solution of H₂O₂.

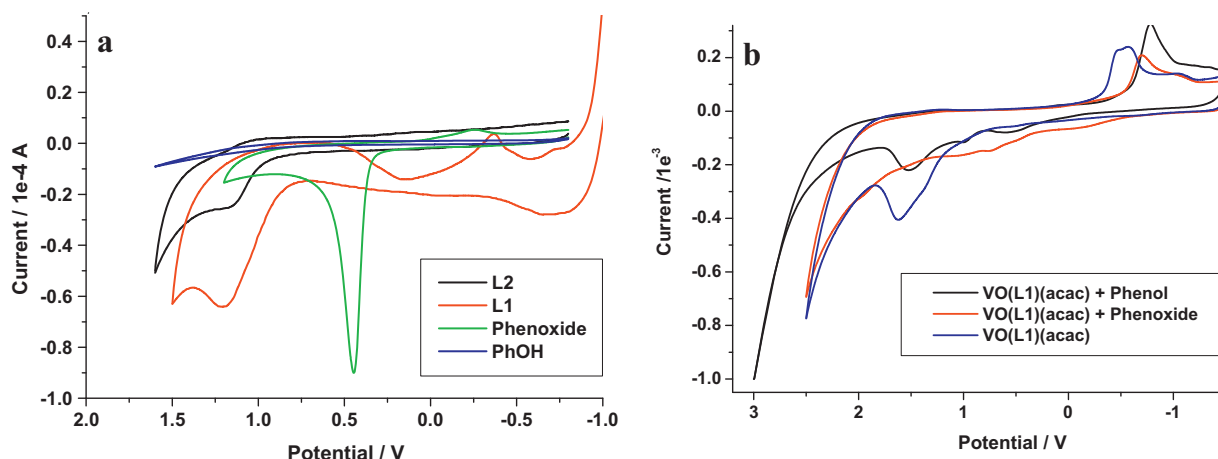


Fig. 11. Cyclic voltammograms of (a) HL^1 , HL^2 , phenol and phenoxide ion (b) $\text{VO}(\text{L}^1)(\text{acac})$ (0.01 M) in MeCN , $\text{VO}(\text{L}^1)$ in presence of phenoxide and phenol in dry acetonitrile in 0.1 M LiClO_4 solution (scan rate 100 mV/s).

Similarly, drop wise addition of H_2O_2 dissolved in MeOH to a 10^{-4} M methanolic solution of $\text{VO}(\text{L}^2)$ resulted in an immediate decrease in intensity of the strong band at 303 nm which disappeared after the second addition of H_2O_2 . The peak at 270 nm becomes more distinguishable from the other bands after the immediate addition of H_2O_2 with a considerable increase in the intensity. Thereafter it decreased with further addition of H_2O_2 . The changes in the electronic spectrum of $\text{VO}(\text{L}^2)$ upon reaction with H_2O_2 in methanol, is shown in Fig. 10b.

The same pattern in the visible region was also observed with $\text{VO}(\text{L}^2)$ (inset Fig. 10b). From the evidence of these kinetic studies, suggests the oxidation of oxovanadium(IV) complex to give oxoperoxovanadium(V) species [39]. Oxoperoxovanadium (V) complexes are very active intermediate species and participate in oxidation reactions by transferring one of its oxygens to the substrate [19,40].

3.4. Electrochemistry and electrocatalysis

Catalyzed electrochemical-oxidation of the oxovanadium complexes were investigated using the cyclic voltammetry technique. The current voltage characteristics were recorded in blank runs for phenol and sodium phenoxide (0.01 M) dissolved in water. Modification in the nature and position of the oxidation waves of the substrate in the presence of the catalyst were carefully recorded. The electrochemical behaviour of the neat complexes was studied in the presence of phenoxide ion (Fig. 11). Behaviour of the phenoxide complexes is unlike that of sodium phenoxide which show irreversible oxidation at $E_{\text{p},\text{a}}$ 0.46 versus Ag/AgCl , under identical conditions. The cyclic voltammogram for $\text{VO}(\text{L}^1)(\text{acac})$ and $\text{VO}(\text{L}^2)$ in acetonitrile exhibit an irreversible peak oxidation wave at 1.62 and 0.73 V, respectively (Fig. 11).

From Fig. 11, it is clear that ligand voltammograms did not show any change while marked shift in oxidation peak were observed for oxovanadium complexes with coordinating phenoxide ions. Furthermore, phenol did not display any electrode process up to a potential of 2.0 V over the glassy carbon electrode in dry acetonitrile, nor even in the presence of the complexes. Hence it was concluded that the presence of the phenoxide ion was essential for the catalysis process. It is likely that the oxidative electron transfer occurs through phenoxide coordinated species. It could be established that the presence of the complexed species facilitated the oxidation process [41].

The electrochemistry of $\text{VOL}^x\text{-Y}$ in acetonitrile is difficult to study because of its low solubility and probably very low percent

loading of metal complexes, and for this reason a carbon paste electrode was used.

4. Conclusion

In this research, oxovanadium(IV) Schiff-base complexes are encapsulated in the nanopores of H-Y zeolites using the flexible ligand method. Encapsulated complexes exhibit fairly clear evidence in the physico-chemical (XRD, BET) and spectral studies (FTIR, UV) for the well-defined inclusion and distribution of complexes in the nanopores of the zeolite matrix. It was found that the encapsulated oxovanadium(IV) catalysts are efficient catalysts for oxidation of cyclohexene with H_2O_2 and reasonably good for oxidation of phenol and benzene, but weakly active for oxidation of styrene. This can be ascribed to a large extent due to shape selective effects in zeolite pores not allowing the relatively large substrates to access catalytic centres easily and for products exit from the channels freely. Oxidation of benzene (<12% conversion) gives phenol with 100% selectivity. For all reactions tested, a high selectivity in competitive reactions is observed, which is correlated to molecular sieving effects (reactants size, selectivity effect). It can be unambiguously seen from the controlled experiments that oxovanadium(IV) species are indeed the active centre and transition metal ions do not play any major role. Results show that the homogeneous catalytic system is more active in the case of phenol, benzene, cyclohexene and styrene having advantages of higher conversions and shorter reaction times than the heterogeneous catalysts. Encapsulated complexes, however, can be recovered and reused without loss of catalytic activity making them better than their neat analogues. The greater stability is due to the suppression of dimeric and other polymeric oxo complexes of VO(IV) attributed to geometric constraints on their formation on encapsulation in zeolites. These results, together with spectral analyses, suggest that interaction between the catalyst and hydrogen peroxide gives rise to peroxovanadium(V) intermediate species which are responsible for transfer of oxygen atoms to the substrates.

References

- [1] J.C. Chadwick, R. Duchateau, Z. Freixa, P.W.N.M. van Leeuwen, *Homogeneous Catalysts: Activity–Stability–Deactivation*, Wiley-VCH, Weinheim, 2011; G.W. Parshall, S.D. Ittel, *Homogeneous Catalysis: The Applications and Chemistry of Catalysis by Soluble Transition Metal Complexes*, second ed., Wiley & Sons, New York, 1992.
- [2] R. Van de Coevering, R.J.M. Klein Gebbink, G. van Koten, *Prog. Polym. Sci. Prog. Polym. Sci.* 30 (2005) 474–490.

- [3] G.A. Ozin, C. Gil, *Chem. Rev.* 89 (1989) 1749–1764;
C.R. Jacob, S.P. Varkey, P. Ratnasamy, *Microporous Mesoporous Mater.* 22 (1998) 465–474.
- [4] R.A. Sheldon, H. van Bekkum, *Fine Chemicals Through Heterogeneous Catalysis*, Wiley-VCH, Weinheim, 2001;
J. Cejka, A. Corma, S. Zones, *Zeolite and Catalysis: Synthesis, Reaction and Applications*, Wiley-VCH, Weinheim, 2010.
- [5] H.J. Neuburg, J.M. Basset, W.F. Graydon, *J. Catal.* 25 (1972) 425–433.
- [6] R.M. Martín-Aranda, J. Cejka, *Top. Catal.* 53 (2010) 141–153.
- [7] J. Cejka, S.P. Mintova, *Catal. Rev. Sci. Eng.* 49 (2007) 457–509.
- [8] J.C. Medina, N. Gabriunas, A. Paez-Mozo, *J. Mol. Catal.* 115 (1997) 233–239.
- [9] M.M. Bhadbhade, D. Srinivas, *Inorg. Chem.* 32 (1993) 5458–5466.
- [10] D.C. Bailey, S.H. Langer, *Chem. Rev.* 81 (1981) 109–148;
B.C. Gates, *Stud. Surf. Sci. Catal.* 29 (1986) 415–425.
- [11] D.C. Crans, J.J. Smee, E. Gaidamauskas, L. Yang, *Chem. Rev.* 104 (2004) 849–902.
- [12] V. Conte, F.D. Furia, G. Licini, *Appl. Catal. A: Gen.* 157 (1997) 335–361.
- [13] A.G.J. Ligtenborg, R. Hage, B.L. Feringa, *Coord. Chem. Rev.* 237 (2003) 89–101.
- [14] C.R. Jacob, S.P. Varkey, P. Ratnasamy, *Appl. Catal. A: Gen.* 168 (1998) 353–364.
- [15] M.R. Maurya, M. Kumar, S.J.J. Titinchi, H.S. Abbo, S. Chand, *Catal. Lett.* 86 (2003) 97–105.
- [16] H.S. Abbo, S.J.J. Titinchi, *Appl. Catal. A: Gen.* 356 (2009) 167–171.
- [17] T.A. Alsallim, J.S. Hadi, O.N. Ali, H.S. Abbo, S.J.J. Titinchi, *Chem. Central J.* 7 (2013) 3.
- [18] T.A. Alsallim, J.S. Hadi, E.A. Al-Nasir, H.S. Abbo, S.J.J. Titinchi, *Catal. Lett.* 136 (2010) 228–233.
- [19] H.S. Abbo, S.J.J. Titinchi, *Top. Catal.* 53 (2010) 1401–1410;
M.R. Maurya, S.J.J. Titinchi, S. Chand, *J. Mol. Catal. A: Chem.* 214 (2004) 257–264;
M.R. Maurya, S.J.J. Titinchi, S. Chand, *J. Mol. Catal. A: Chem.* 201 (2003) 119–130;
M.R. Maurya, S.J.J. Titinchi, S. Chand, *J. Mol. Catal. A: Chem.* 193 (2003) 165–176;
M.R. Maurya, S.J.J. Titinchi, S. Chand, *Catal. Lett.* 89 (2003) 219–227;
M.R. Maurya, S.J.J. Titinchi, S. Chand, *Appl. Catal. A: Gen.* 228 (2002) 177–187.
- [20] G. Bett, D.E. Fenton, J.R. Tate, *Inorgan. Chim. Acta* 54 (1981) L101–L102.
- [21] J.-P. Costes, G. Crcs, M.-H. Darbieu, J.-P. Laurent, *Inorg. Chim. Acta* 60 (1982) 111–114.
- [22] L.J. Boucher, E.C. Tynan, T.F. Yen, *Inorg. Chem.* 7 (1968) 731–736.
- [23] L.F. Vilas Boas, J. Costa Pessoa, in: G. Wilkinson, R.D. Gillard, J.A. McCleverty (Eds.), *Comprehensive Coordination Chemistry*, 3, Pergamon Press, Oxford, 1987, pp. 453–583.
- [24] M. Goodgame, P.J. Hayward, *J. Chem. Soc. A* (1966) 632–634.
- [25] K.B. Kusum, C.D. Ramesh, *J. Phys. Chem. C* 116 (2012) 14295–14310.
- [26] M.R. Maurya, S.J.J. Titinchi, S. Chand, I.M. Mishra, *J. Mol. Catal. A: Chem.* 180 (2002) 201–209.
- [27] H.S. Abbo, S.J.J. Titinchi, *Top. Catal.* 53 (2010) 254–264.
- [28] C.J. Ballhausen, H.B. Gray, *Inorg. Chem.* 1 (1962) 111–122.
- [29] C.R. Cornman, K.M. Geiser-Bush, S.P. Rowley, P.D. Boyle, *Inorg. Chem.* 36 (1997) 6401–6408.
- [30] G. Meyer, D. Woehrle, M. Mohl, G. Schulz-Ekloff, *Zeolites* 4 (1984) 30–34;
H. Diegruber, P.J. Plath, G. Schulz-Ekloff, M. Mohl, *J. Mol. Catal.* 24 (1984) 115–126.
- [31] S.P. Varkey, C. Ratnasamy, P. Ratnasamy, *J. Mol. Catal. A: Chem.* 135 (1998) 295–306.
- [32] H.S. Abbo, S.J.J. Titinchi, *Appl. Catal. A: Gen.* 435–436 (2012) 148–155;
S.J.J. Titinchi, H.S. Abbo, *Catal. Today* 204 (2013) 114–124;
H.S. Abbo, S.J.J. Titinchi, R. Prasad, S. Chand, *J. Mol. Catal. A: Chem.* 225 (2005) 225–232;
M.R. Maurya, I. Jain, S.J.J. Titinchi, *Appl. Catal. A: Gen.* 249 (2003) 139–149.
- [33] S.M. Csicsery, *Zeolites* 4 (1984) 202–213.
- [34] W.F. Holderich, H. van Bekkum, *Zeolite and related materials in organic syntheses. Bronsted and Lewis catalysis*, in: H. van Bekkum, E.M. Flanigen, P.A. Jacobs, J.C. Jansen (Eds.), *Introduction to Zeolite Science and Practice*, Elsevier, Amsterdam, 2001, p. p839;
S.-C. Sujandi, D.-S. Han, M.-J. Han, S.-E. Jin, Park, *J. Catal.* 243 (2006) 410–419;
J.D. Bass, A. Solov'yov, A.J. Pascall, A. Katz, *J. Am. Chem. Soc.* 128 (2006) 3737–3747.
- [35] I. Kuz'niarska-Biernacka, A.M. Fonseca, I.C. Neves, *Inorg. Chim. Acta* 394 (2013) 591–597.
- [36] V. Hulea, E. Dumitriu, *Appl. Catal. A: Gen.* 277 (2004) 99–106.
- [37] M.R. Maurya, M. Kumar, A. Kumar, J.C. Pessao, *Dalton Trans.* (2008) 4220–4232.
- [38] I. Kuz'niarska-Biernacka, K. Biernacki, A.L. Magalhães, A.M. Fonseca, *J. Catal.* 278 (2011) 102–110.
- [39] C.R. Waidmann, A.G. DiPasquale, J.M. Mayer, *Inorg. Chem.* 49 (2010) 2383–2391.
- [40] P. Adao, J. Costa Pessoa, R.T. Henriques, M.L. Kuznetsov, F. Avecilla, M.R. Maurya, U. Kumar, I. Correia, *Inorg. Chem.* 48 (2009) 3542–3561.
- [41] H.S. Abbo, S.J.J. Titinchi, S. Chand, R. Prasad, *J. Mol. Catal. A: Chem.* 218 (2004) 125–132.